Automated analysis of XANES: A feasibility study of Au reference compounds

2016 J. Phys.: Conf. Ser. 712 012070

(http://iopscience.iop.org/1742-6596/712/1/012070)

Journal of Physics: Conference Series **712** (2016) 012070 doi:10.1088/1742-6596/712/1/012070

Automated analysis of XANES: A feasibility study of Au reference compounds

S-Y Chang[1,2], L B Molleta[1], S G Booth[1], A Uehara[1,4], J F W Mosselmans[2], K Ignatyev[2], R A W Dryfe[1], S L M Schroeder[1-3]*

[1]School of Chemistry and School of Chemical Engineering and Analytical Science, University of Manchester, M13 9PL Manchester, UK.

[2]Diamond Light Source Ltd, Didcot, OX11 0DE Oxfordshire, UK.

[3]School of Chemical and Process Engineering, University of Leeds, Leeds LS2 9JT, UK.

[4]Division of Nuclear Engineering Science, Research Reactor Institute, Kyoto University, Asashironishi, Kumatori, Osaka, 590-0494, Japan.

*Email: s.l.m.schroeder@leeds.ac.uk

Abstract With the advent of high-throughput and imaging core level spectroscopies (including X-ray absorption spectroscopy, XAS, as well as electron energy loss spectroscopy, EELS), automated data processing, visualisation and analytics will become a necessity. As a first step towards these objectives we examined the possibilities and limitations of a simple automated XANES peak fitting procedure written in MATLAB, for the parametrisation of XANES features, including ionisation potentials as well as the energies and intensities of electronic transitions. Using a series of Au L_3-edge XANES reference spectra we show that most of the relevant information can be captured through a small number of rules applied to constrain the fits. Uncertainty in this strategy arises mostly when the ionisation potential (IP) overlaps with weak electronic transitions or features in the continuum beyond the IP, which can result in ambiguity through multiple equally good fits.

1. Introduction

Core level spectroscopies such as electron energy loss spectroscopy (EELS) and X-ray absorption spectroscopy (XAS) provide element specific chemical information. The robustness of these spectroscopies has enabled their use across a broad range of applications, including for example oil, gas, nuclear fuel and waste processing research, materials science, electrochemistry, crystallisation, biological and geochemical speciation as well as conservation and restoration of heritage objects. A current trend is to develop high-throughput functionality, which will enable exploration of more applications for these spectroscopies. Some imaging [3-5] and quick scanning EXAFS facilities [6-8] are already providing hundreds and thousands of XANES spectra within minutes to hours. As such, it would be useful to have access to algorithms that permit an initial assessment of such datasets by automated parametrisation for subsequent classification. This would also pave the way to a fuller interpretation of chemical contrast in XANES images.

The fine-structure features in the near-edge region of EELS and XAS (inclusive of XANES and NEXAFS) arise from electronic transitions to bound states and thus contain rich information about the local structure and the chemical state of the probed element. XANES spectra of transition metals are

often used for fingerprinting and to determine the oxidation state and coordination geometry (e.g., octahedral vs. tetrahedral) from known spectral characteristics [9]. We have already shown that through deconvolution (peak fitting) of spectral features and subsequent assignment of bound state transitions to these features the interactions of small organic molecules such as protonation, intermolecular solvent-solute hydrogen bonding and solute-solute interaction can be studied in detail [10, 11]. In fact, peak fitting is the only way to determine energies, intensities and widths of the most prominent absorption features.

Functional peak fitting programs for XANES analysis are currently available [12-16], but to enable automated fitting of large numbers of spectra reliable principles allowing both flexibility and robustness are required. The increasing need to process larger numbers of spectra has led us to explore the use of an automated peak fitting procedure based on a simple heuristic approach to obtain the energetic positions and intensities of XANES absorption features by use of a MATLAB script. It builds on the use of a script we recently reported as part of a time-resolved quick EXAFS study of Pd nucleation [17]. In this work we discuss the possibilities and limitations of such an approach by reference to a set of Au L_3-edge XANES spectra from various reference compounds. We would like to stress that the aim of this work was not to provide a definite general XANES fitting tool, but to explore the possibilities and limitations of using a few heuristic rules to constrain an automated fitting procedure.

2. The Peak Fitting Algorithm

We focused on the parametrisation of the XANES region based on the determination of energies, intensities and widths of the most prominent features. For this we chose to simulate any absorption feature below the ionisation potential (IP) with pseudo-Voigt functions [18, 19], while the absorption edge jumps/IPs were modelled using error functions [15]. This represented a pragmatic and heuristic choice based on our finding that this combination fitted most reference spectra well. In the energy region from just below to slightly above the IP, absorption features due to electronic transitions overlap with EXAFS and multiple scattering features such as shape resonances. Fine structure beyond the IP and in the continuum was modelled using Gaussian peak functions, but we stress that this was done only to remove the EXAFS background which extends into the XANES region, to increase the reliability of the fits of interest in the XANES region, and not to analyse or parametrise the EXAFS part of the spectrum. These Gaussian components of the fits have no physical meaning.

To optimise the fit a MATLAB default trust-region-reflective algorithm was applied, as this method allows boundary limits to be specified. The variables to be optimised during fitting were the number of absorption features to model and then for each fitted function the full width at half maximum (FWHM), the centroid energy, the area and for pseudo-Voigt functions, the Lorentzian/Gaussian ratio η. Using an arctangent instead of an error function resulted in slightly different but still consistent results for IP positions and the absorption features related to transitions to bound states (not shown), albeit with overall worse fit quality. Energy boundaries and constraints were imposed to ensure that the automated fitting results retained physical meaning.

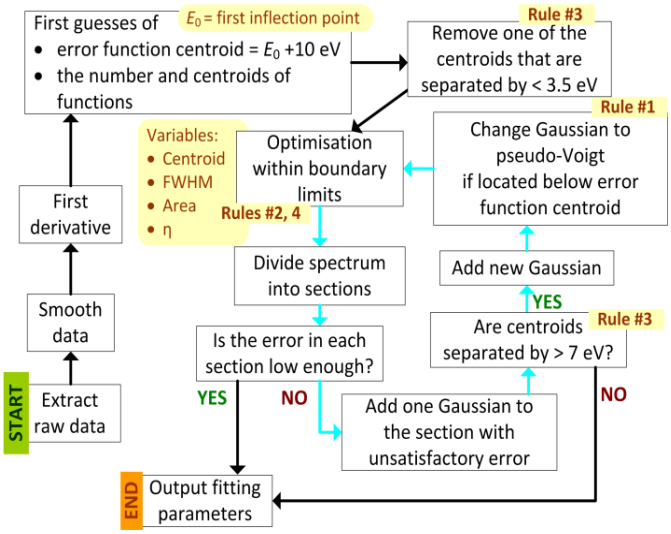

Figure 1. The peak fitting algorithm

In other words, by constraining the fits with a few heuristic 'rules', the parameter landscape available for an automated fit was reduced considerably, reflecting prior knowledge about relationships between XANES absorption features, chemical state and local structure.

To start with, we assumed that any absorption maximum located at a lower energy than the step function modelling the IP must correspond to the excitation of a core electron to an unoccupied bound electronic state (Rule #1). In order to determine the FWHM for the error function and the pseudo Voigt functions an initial guess and lower boundary limit was obtained from tabulated natural line width data [20]. These are independent of the electronic structure in the valence region (Rule #2). By way of example, in the samples examined here the natural line width for Au L_3 is 5.41 eV therefore the allowable range in the subsequent fitting error function was constrained from 5.41 eV to 10 eV and for the pseudo-Voigt functions from 5.41 eV to 15.41 eV. Rule #3 imposes that electronic transitions must be separated from each other by a threshold value, to prevent overfitting, e.g. 3.5 eV for the initial guess (grey arrows, figure 1) and 7 eV for the subsequent guess (blue arrows, figure 1) gave good results for all Au L_3-edge spectra. Aside from the FWHM limit in Rule #2, the height of the IP error functions was fixed at 0.8 for all the Au L_3-edge spectra to enable the use of the non-negative Gaussian functions to fit oscillatory fine structure in the continuum range (Rule #4). For the set of data discussed here the FWHM of the electronic transition features tends to increase with photon energy due to increased lifetime broadening [21]. If necessary in a specific data set this trend could also be imposed as Rule #5.

The resulting algorithm is summarised in figure 1. In a first optimisation loop, the number of peaks to be fitted and their centroids are guessed from the first derivative of the smoothed experimental spectrum. A peak centroid is then assigned to each maximum in the spectrum. The initial guess for the IP is the edge inflection point of the experimental spectrum (E_0) + 10 eV. In the subsequent minimisation loop (blue arrows in figure 1) the difference between the experimental spectrum and the fitted line shapes is examined, and Gaussians are added where the deviation between experiment and fit is larger than a threshold value, while maintaining Rules #1 and #3.

3. Results and Discussion

The peak fitting algorithm was tested on a series of Au L_3-edge reference spectra. Fitting each spectrum using the code took at most a few seconds on a computer with a first generation Intel i3 processor. For comparison, we also generated manual (non-automatic) best fits for all spectra using Athena in the Demeter software package [13]. The full experimental methodology, results and the MATLAB code are given in the supporting information (SI).

For gold foil, $[AuCl_2]^-$ and Au_2S, good agreement was achieved between automatic and manual best fits (figure 2) producing similar error and pseudo-Voigt function parameters in the XANES region. For $[Au(CN)_2]^-$, $[Au(CN)_4]^-$ and $[AuCl_4]^-$, similarly good agreement in the XANES region can be achieved, although with more than one way to fit the data. For $[Au(CN)_4]^-$, both the automatic fit with three pseudo-Voigt functions and the manual fit with two pseudo-Voigt functions seem equally reasonable. For $[Au(CN)_2]^-$ and $[AuCl_4]^-$, the manual best fits model the regions around 11,930 and 11,926 eV, respectively, better because a weak secondary pseudo-Voigt function improves the fit. The contribution of this transition was too low to be picked up by the automated algorithm. The parameters determined for the strong white line and the IP in these examples are still in good enough agreement to be of analytical value. A similar situation was encountered for $[AuBr_4]^-$ (SI B). A similar but more severe case is $[Au(OH)_4]^-$, which has a secondary and even what appears to be weak tertiary contribution to the white line just below the IP, which are not correctly identified by the automated algorithm.

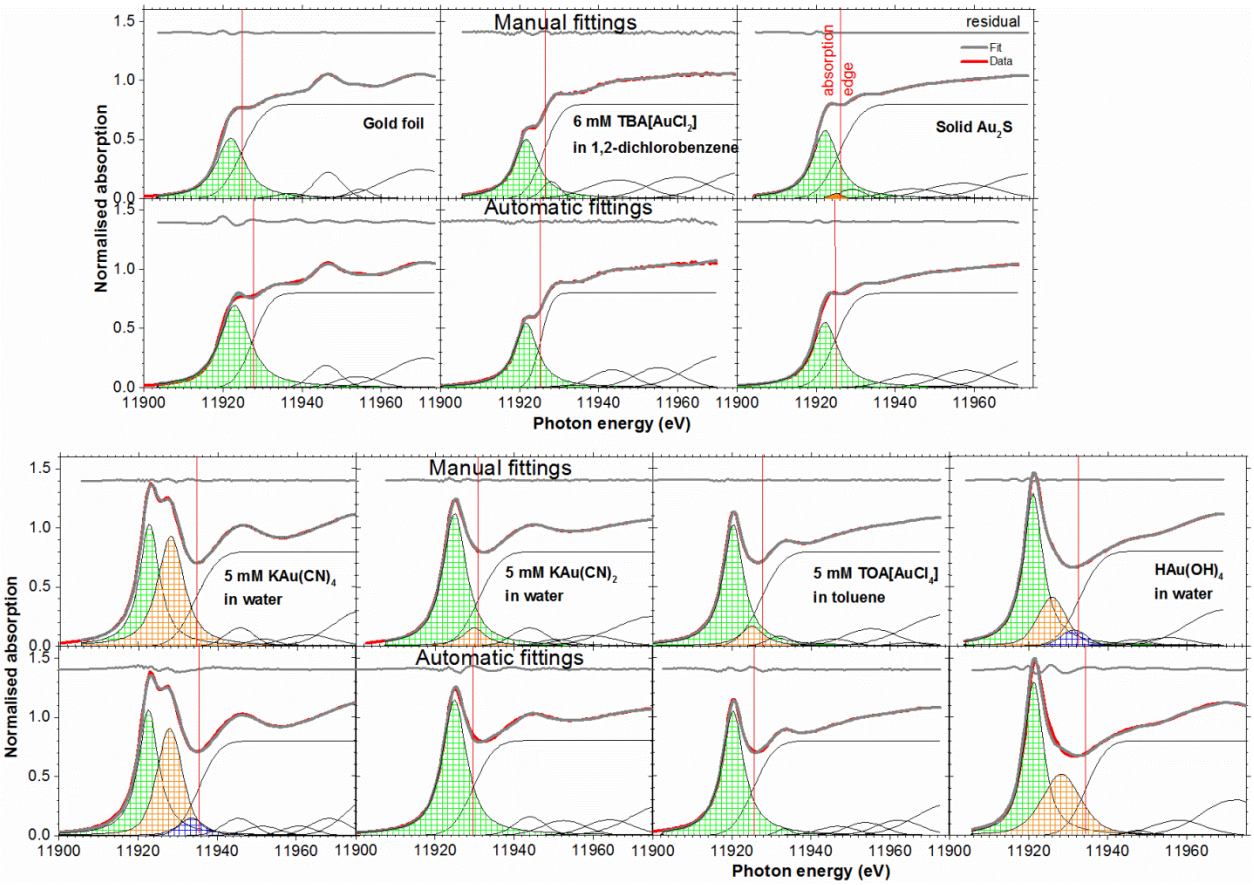

Figure 2. The automatic fits in comparison with the manual fits. The pseudo-Voigt functions were shaded in different colours to contrast between the first (green), second (orange) and third (blue) functions. Au_2S, $[AuCl_2]^-$ and $[Au(OH)_4]^-$ spectra were obtained from references [1, 2].

4. Conclusions

The heuristic automated peak fitting procedure parametrises most of the essential electronic structure and chemical state information at the Au L_3-edge with minimal user input. For the test set of Au L_3-edge XANES spectra the fits were excellent for most of the compounds while for others some further refinement is required through inclusion of secondary white line features. The method has the flexibility to be applied to different edges through the use of the necessary edge-specific boundary limits. We plan to implement the method in a more open language such as Python. We believe that such simple automation procedures will already be useful for the initial stages of data analysis for large bodies of spectra, e.g. filtering and classification of datasets or interpreting chemical contrast in imaging data more quantitatively. Through further advancement of this technique the methodology could ultimately also be linked with molecular modelling and simulation for deeper understanding of the variations in peak positions and intensities in the XANES region.

Acknowledgements

All data supporting this study are provided either in the results section of this paper or in the supplementary information accompanying it. The authors acknowledge the Diamond Light Source beamtime on I18 awarded under proposal SP-8861. RAWD and SLMS acknowledge support through an EPSRC-NSF "Materials World Network" grant (EP/H047786/1). SLMS thanks EPSRC for financial support under the critical mass grant EP/I013563/1. AU thanks Kyoto University foundation for supporting a sabbatical visit to UoM. SYC gratefully acknowledges UoM, and Mr and Mrs Clews

for the Robert Clews Presidential sponsorship, as well as the Royal Society of Chemistry and XAFS16 for conference travel grants.

References

[1] Lengke M F, Ravel B, Fleet M E, Wanger G, Gordon R A and Southam G 2007 *Can. J. Chem.* **85** 651-59
[2] Chang S-Y, Uehara A, Booth S G, Ignatyev K, Mosselmans J F W, Dryfe R A W and Schroeder S L M 2015 *RSC Adv.* **5** 6912-18
[3] Scott R A, Shokes J E, Cosper N J, Jenney F E and Adams M W W 2005 *J. Synchrotron Rad.* **12** 19-22
[4] Fischer D, Jaye C, Scammon K, Sobol P and Principe E 2010 *Microsc. Microanal.* **16** 380-81
[5] Cueva P, Hovden R, Mundy J A, Xin H L and Muller D A 2012 *Microsc. Microanal.* **18** 667-75
[6] Baudelet F, Kong Q, Nataf L, Cafun J D, Congeduti A, Monza A, Chagnot S and Itié J P 2011 *High Pressure Res.* **31** 136-39
[7] Frahm R, Nachtegaal M, Stötzel J, Harfouche M, van Bokhoven J A and Grunwaldt J-D 2010 The Dedicated QEXAFS Facility at the SLS: Performance and Scientific Opportunities *10th International Conference on Radiation Instrumentation*: *AIP Conf. Proc.* (*Melbourne, Australia, 27 September–2 October 2009)* ed R. Garrett, I. Gentle, K. Nugent, and S. Wilkins pp 251-55
[8] Belin S, Briois V, Traverse A, Idir M, Moreno T and Ribbens M 2005 *Phys. Scripta*. **2005** 980
[9] Yamamoto T 2008 *X-Ray Spectrom.* **37** 572-84
[10] Thomason M J, Seabourne C R, Sattelle B M, Hembury G A, Stevens J S, Scott A J, Aziz E F and Schroeder S L M 2015 *Faraday Discuss.* **179** 269-89
[11] Stevens J S, Seabourne C R, Jaye C, Fischer D A, Scott A J and Schroeder S L M 2014 *J. Phys. Chem. B.* **118** 12121-29
[12] Wojdyr M 2010 *J. Appl. Crystallogr.* **43** 1126-28
[13] Ravel B and Newville M 2005 *J. Synchrotron Rad.* **12** 537-41
[14] Newville M 2013 Larch: An Analysis Package for XAFS and Related Spectroscopies *15th International Conference on X-ray Absorption Fine Structure (XAFS15)*: *J Phys. Conf. Ser.* (*Beijing, China, 22-28 July 2012)* ed Z. Wu pp 012007
[15] Boubnov A, Lichtenberg H, Mangold S and Grunwaldt J-D 2015 *J. Synchrotron Rad.* **22** 410-26
[16] Delgado-Jaime M U, Mewis C P and Kennepohl P 2010 *J. Synchrotron Rad.* **17** 132-37
[17] Chang S-Y, Gründer Y, Molleta L B, Uehara A, Mosselmans J F W, Cibin G, Dryfe R A W and Schroeder S L M 2016 *CrystEngComm*. **18** 674-82
[18] Amemiya K, Kitajima Y, Yonamoto Y, Terada S, Tsukabayashi H, Yokoyama T and Ohta T 1999 *Phys. Rev. B.* **59** 2307-12
[19] Stohr J 2003 *NEXAFS Spectroscopy* Springer series in surface sciences vol. 25, ed R. Gomer (Heidelberg: Springer-Verlag)
[20] Krause M O and Oliver J H 1979 *J. Phys. Chem. Ref. Data*. **8** 329-38
[21] Bunker G 2010 *Introduction to XAFS: A Practical Guide to X-ray Absorption Fine Structure Spectroscopy* (New York: Cambridge University Press)